Journal of Applied Mechanics and Technical Physics, Vol. 44, No. 4, pp. 471–481, 2003

RELAXATION-INDUCED SUPPRESSION OF VORTEX DISTURBANCES IN A MOLECULAR GAS

Yu. N. Grigor'ev[1] **and I. V. Ershov**[2]

UDC 532.5:532.517.4

The influence of thermal excitation on a finite-amplitude vortex disturbance in a shear flow of a molecular gas is studied in a model problem. The evolution of such vortex structures is typical of both the nonlinear stage of the laminar–turbulent transition and for developed turbulence. Since the excitation level was assumed to be comparatively low, full Navier–Stokes equations for a compressible heat-conducting gas were used in calculations; nonequilibrium was taken into account by the coefficient of bulk viscosity. As the bulk viscosity increases in the range of realistic values, the disturbance-energy damping rate in a weakly compressible flow increases approximately by 10%. The increase in the Mach number enhances the effect of disturbance suppression.

Key words: *vortex disturbances, molecular gas, relaxation, suppression.*

Introduction. Lately, the development of new methods for influencing the processes of the laminar–turbulent transition and turbulence generation became a subject of considerable attention. The investigation is focused on effects earlier neglected by specialists in hydrodynamics. One possible method for acting on a compressible molecular gas flow is based on an additional dissipative effect arising during relaxation of internal molecular degrees of freedom. This effect is manifested, for instance, in the form of anomalous absorption of ultrasound in molecular gases, which was first observed and physically interpreted in 1930s (see [1]). In supersonic flows, nonequilibrium distributions of internal molecular energy often occur naturally, for example, in nozzles, in nonisobaric jets, and behind oblique shock waves. In the hydrodynamic approximation, this dissipative process corresponds to the bulk viscosity coefficient in the stress tensor [2]. Mack [3] was the first to introduce bulk viscosity in the equations of the theory of stability of a compressible boundary layer (CBL). Up to now, however, the influence of bulk viscosity or, in the general case, relaxation of internal degrees of freedom on CBL stability has not been investigated in sufficient detail.

Nerushev and Novopashin [4] describe comparative experiments on the laminar–turbulent transition in a Poiseuille flow in a round tube for nitrogen N_2 and carbon oxide CO. The thermodynamic and transport properties of these gases are almost identical, but the bulk viscosity of CO calculated from the data on ultrasound attenuation is several times greater than a similarly parameter for N_2. It is experimentally established that, other conditions being identical, the transition Reynolds number Re_t in more "viscous" CO is approximately 10% higher than the respective figure for N_2. Such a change in Re_t is essential because its order of magnitude is comparable with that of the practically applied mechanical methods for drag reduction [5]. Although the results obtained are disputable, at least, they are worthy of theoretical verification and analysis, all the more so because previous investigators of hydrodynamic stability and laminar–turbulent transition had not considered this effect. Certainly, the data on ultrasound attenuation suggest that high-frequency fluctuations are more intensively suppressed in a gas with a higher bulk viscosity. These data, however, involve frequencies of several megahertz, whereas the proportion of disturbance energy in this part of the spectrum is negligibly small even in supersonic flows.

[1]Institute of Computational Technologies, Siberian Division, Russian Academy of Sciences, Novosibirsk 630090. [2]Novosibirsk State Academy of Water Transport, 630099 Novosibirsk. Translated from Prikladnaya Mekhanika i Tekhnicheskaya Fizika, Vol. 44, No. 4, pp. 22–34, July–August, 2003. Original article submitted October 24, 2002; revision submitted December 11, 2002.

Bertolotti in his work [6] partially inspired by the publication [4] was the first to investigate in detail the impact of nonequilibrium of internal degrees of freedom on the laminar–turbulent transition. The CBL stability on a semi-infinite plate was considered for atmospheric flight conditions at an altitude $H = 12$ km with a Mach number $M_\infty = 4.5$. The selected mode corresponds to the motion of real objects in the case where there is no dissociation in the near-wall flow but internal degrees of freedom of oxygen and nitrogen molecules are significantly excited. In calculations, the nonequilibrium of rotational and vibrational degrees of freedom was assumed to occur naturally. In particular, it was considered that the equilibrium energy distribution is violated because of the acceleration of air in the nozzle up to the design Mach number if the flight is simulated in a wind tunnel and because of the flow acceleration behind an oblique shock wave on the blunted leading edge of the plate if the motion occurs in undisturbed atmosphere. Calculations based on the equations of the linear stability theory showed that the allowance for bulk viscosity results in an insignificant stabilizing effect reducing the amplitude of the second instability mode by several percent only. (Note, the definitions of the first and second instability modes in CBL, first discovered in [3], can be found in [7].) Depending on temperature, the ratio of bulk viscosity μ_b and dynamic viscosity μ changed within the range $\alpha = \mu_b/\mu = 0.6$–1.0 typical of air.

A much stronger and unexpectedly destabilizing effect was observed with a significant deviation from equilibrium, which can no longer be described by the bulk viscosity model. From the calculations of CBL stability for a wind-tunnel experiment on a flat plate with a sharp leading edge, it follows that the amplitude of low-frequency disturbances of the first instability mode is approximately 50 times as great as the calculation results based on the thermal equilibrium assumption. Because of the shift of the upper branch of the neutral stability curve, the region of the first instability mode proves to be significantly expanded downstream. The calculation results for a blunted plate moving in an undisturbed atmosphere with allowance for nonequilibrium behind the shock wave yielded a doubled amplitude of the first mode against the value obtained for equilibrium conditions.

The data presented call for the further study of the effect of thermal nonequilibrium, including artificial nonequilibrium, on the transition in compressible flows. Note that the model of bulk viscosity in [6] is considered for significantly lower values of the parameter α than in the experimental work [4], where the value for CO was estimated as $\alpha \simeq 7$.

The CBL destabilization effect was found outside the applicability area of the bulk viscosity model. In [6], it was attributed to the drastic decrease in the static temperature due to the excess fraction of internal energy remaining in vibrational degrees of freedom upon rapid expansion. It was assumed that, during a characteristic flow time, rotational degrees of freedom promptly come into equilibrium with translational degrees of freedom, and the energy in vibrational degrees of freedom remains frozen. Thus, in this case, the change in CBL stability is not directly related to the impact of the relaxation process. In addition, as was noted in [6], the increase in disturbances, even that exponential in the linear approximation, can be stabilized at the nonlinear stage of the transition. At the same time, Nerushev and Novopashin in [4] studied the nonlinear stage of the transition to the turbulent regime because the Hagen–Poiseuille flow is stable in the linear approximation.

Within the linear stability theory, the authors of the present paper in their publication [8] estimated the impact of bulk viscosity on CBL stability on a thin plate with a finite chord. For Mach numbers $M \leqslant 10$ and values $\alpha \leqslant 30$, which is really attained for hydrogen [9]; it was found that the contribution of the additional dissipative effect to the change in Re_t does not exceed several tenths of a percent.

The current scenarios of the processes of the laminar–turbulent transition and turbulence generation imply that emergence, evolution, and decay of characteristic vortex structures occur at the nonlinear stage. Various λ-structures (horseshoes and hairpins) are observed in near-wall flows and tube flows, and two-dimensional vortices extended in the transverse direction are observed in plane shear layers and jets. Therefore, turbulence generation can be interpreted as a process of the laminar–turbulent transition, randomly repeatable in space and time. This enables us to assume that the role of bulk viscosity μ_b at the nonlinear stage of disturbance development can be estimated by modeling the interaction of a single organized vortex structure with the main (mean) flow. In the present paper, we consider a simple model of evolution of a transverse vortex structure in the shear layer of a nonequilibrium molecular gas.

1. Model Selection and Parametrization. 1.1. *Bulk Viscosity.* As follows from the kinetic theory of polyatomic gases [10], the method for nonequilibrium description in terms of internal degrees of freedom in the hydrodynamic approximation depends on the degree of deviation from equilibrium. In addition, allowance should be made for the relation between relaxation times of various modes of internal molecular dynamics and the characteristic flow time.

TABLE 1

Gas	$\mu \cdot 10^{-5}$, Pa·sec	$\mu_b^{(s)} \cdot 10^{-5}$, Pa·sec	$\alpha = \mu_b^{(s)}/\mu$	$\mu_b^{(r)} \cdot 10^{-5}$, Pa·sec	$\alpha = \mu_b^{(r)}/\mu$
N_2	1.750	0.348	0.199	0.966	0.552
CO	1.750	12.274	7.014	1.231	0.703
Air	1.820	1.178	0.647	—	—
CO_2	1.460	54.015	39.997	—	—
H_2	0.880	34.570	39.280	—	—

With relatively low levels of thermal excitation, the energy distribution over molecular degrees of freedom is characterized by an identical temperature, and the energy exchange between translational and internal degrees of freedom is taken into account by using the coefficient of bulk viscosity μ_b in the stress tensor P_{ij} in the Navier–Stokes equations, which has the following form in the conventional tensor notation:

$$P_{ij} = p\delta_{ij} - \mu\Big(\frac{\partial u_i}{\partial x_j} + \frac{\partial u_j}{\partial x_i} - \frac{2}{3}\,\delta_{ij}\,\frac{\partial u_k}{\partial x_k}\Big) - \mu_b\delta_{ij}\,\frac{\partial u_k}{\partial x_k}, \quad p = \rho RT. \tag{1}$$

In (1), x_i are Cartesian coordinates, u_i are the respective components of the velocity vector, p, ρ, and T are the static pressure, density, and temperature of the gas, and R is the gas constant. Hereinafter, summation is performed over repeated indices.

In the general case of polyatomic gases, internal energy is distributed over rotational and vibrational modes. In this case, the bulk viscosity coefficient is written as [10]

$$\mu_b = (pR/c_v)(\gamma_r\tau_{r,r} + \gamma_v\tau_{r,v}), \tag{2}$$

where c_v is the specific heat at constant volume, γ_r and γ_v are the fractions of internal energy in rotational and vibrational degrees of freedom, and $\tau_{r,r}$ and $\tau_{r,v}$ are the relaxation times of the corresponding degrees of freedom.

We consider flows with moderate supersonic velocities and a stagnation temperature $T_0 \simeq 1000$ K. In this case, vibrational levels are very weakly excited, and it can be assumed that $\gamma_v \approx 0$. Then, $\gamma_r = 2/5$, and the relaxation time of rotational degrees of freedom is expressed as

$$\tau_{r,r} = Z_r\tau_t, \tag{3}$$

where τ_t is the mean free path of molecules in the gas and Z_r is the coefficient of energy exchange between rotational and translational degrees of freedom [10]. The coefficient Z_r is equal to the average number of intermolecular collisions required for the rotational mode to relax to equilibrium.

Available publications on bulk viscosity of molecular gases fail to provide consistent data and often contradict one another. Earlier results are based on the measurements of ultrasound absorption. In the linear acoustic approximation, the absorption coefficient is given by formula [9] (see also [1])

$$æ = \frac{2\pi\omega^2}{\rho c_s^2}\Big[\frac{4}{3}\,\mu + \mu_b + \frac{\lambda(\gamma-1)}{c_p}\Big]. \tag{4}$$

Here λ is the thermal conductivity, γ is the ratio of specific heats, c_s is the velocity of sound, c_p is the specific heat at constant pressure, and ω is the frequency of an ultrasonic wave.

The values of bulk viscosity $\mu_b^{(s)}$ calculated by formula (4) at $T = 273$ K and $p = 10^5$ Pa are listed in Table 1. The values of the absorption coefficient æ are taken from [9]. Note that the values of æ for N_2 and CO coincide with those published in [4].

At present, the values of μ_b are determined from electron-optical measurements of the relaxation times $\tau_{r,r}$ or exchange coefficients Z_r in shock waves and underexpanded jets. Some values of $\mu_b^{(r)}$ calculated by formulas (2) and (3) using experimental data from the references to [9] are also presented in Table 1. These results are in good agreement with the values of μ_b calculated using various kinetic models and with later data of other authors (see the references to [9, 10]).

The difference in values of $\mu_b^{(s)}$ and $\mu_b^{(r)}$ for CO by an order of magnitude may be attributed to the specific sensitivity of acoustic sensors to infinitesimal impurities in the gas [9]. At the same time, a comparison of the presented values of $\mu_b^{(r)}$ shows that, for the given values of p and T, the bulk viscosity of CO is only by one third higher than the same parameter for N_2. If the values of the coefficients Z_r from [4] are used in (2) and (3), the thus calculated bulk viscosity of nitrogen appears to be two times higher than the value of $\mu_b^{(r)}$ for CO. Nerushev and

Novopashin [4] did not comment this disagreement of the original data, although it contradicts the very idea of the experiment.

The dependence $Z_r(T)$ is calculated by the relations presented in [11], which are in satisfactory agreement with the experimental data and results of direct numerical modeling (see the references in [10]). According to the calculation data (see Table 1), as T increases from 273 to 1000 K, the value of α increases almost twofold.

It can be concluded, therefore, that the ratio of bulk viscosity to shear viscosity is $\alpha \leqslant 2$ for flows of molecular gases with moderate parameters.

1.2. *Flow Parameters.* The influence of bulk viscosity on the laminar–turbulent transition and turbulence generation was estimated by means of a simple model of interaction between a two-dimensional vortex structure and a plane shear flow. Such structures emerge in plane mixing layers, jets, and wakes of bodies in the flow. The Mach number in the main flow is assumed to be $\mathrm{M}_0 < 1$. In this case, the compressibility influence on kinematic and dynamic characteristics of the structure can be neglected, and modeling parameters can be chosen using validated data on mixing layers [12, 13].

The relative intensity of a vortex structure is given by the parameter $\beta = u'/\Delta u \approx v'/\Delta u$ (u' and v' are the maximum velocity fluctuations and Δu is the absolute difference in velocities on the mixing layer boundaries). According to [12] (see also [13]), $\beta \simeq 0.2$–0.5.

Intermittency in the streamwise direction is given by the relation of the vortex size R_0 to the half-distance between the structures $l/2$. On the average, for mixing layers and jets, the intermittency coefficient is $\chi = l/(2R_0) = 2$–6. The characteristic relation between the layer thickness δ and the structure size is estimated as $\delta/R_0 \simeq 2$–4 [12, 13].

It follows from experimental data and calculations (see [12] and references to it) that the dynamics of all disturbances, including large-scale structures, is universal in mixing layer for Reynolds numbers $\mathrm{Re} = \rho\Delta u\delta/\mu \geqslant 10^2$. For this reason, calculations can be performed for moderate Reynolds numbers, thus, avoiding certain computational difficulties.

In choosing the velocity profile of the carrier jet, the Tollmien solution [13] was applied to the mixing layer on the jet boundary. In self-similar variables, the streamwise velocity profile in the layer has the form

$$\bar{u}_T = u(\varphi)/(2U_0) = F'(\varphi) = 0.0176\mathrm{e}^{-\varphi} + 0.6623\cos(\sqrt{3}\varphi/2) + 0.2280.\mathrm{e}^{\varphi}\sin(\sqrt{3}\varphi/2), \tag{5}$$

where $\varphi = x_2/(ax_1)$ and a is an empirical constant characterizing the layer structure. The function $F'(\varphi)$ is tabulated in [13]. For $\varphi_0 = 0.98$, profile (5) is conjugated with the jet core, where $F'(\varphi_0) = 1$ and $u(\varphi_0) = 2U_0$. The value of $\varphi_n = -2.04$ corresponds to the external boundary of the jet, where $F'(\varphi_n) = 0$. The linear velocity profile between these values is given by the formula

$$\bar{u}_l = u/(2U_0) = (\varphi - \varphi_n)/(\varphi_0 - \varphi_n). \tag{6}$$

A comparison of profiles (5) and (6) shows that the root-mean-square deviation

$$\sigma = \sqrt{\frac{1}{n}\sum_{i=1}^{n}(\bar{u}_T(\varphi_i) - \bar{u}_l(\varphi_i))^2}$$

does not exceed $\sigma = 0.075$. This proves the feasibility of modeling the carrier stream by a linear shear flow.

If the structure center is considered to be located on the mid-streamline and moves with a velocity U_0, we can pass to the system of coordinates where it is at rest. The Rankine vortex of radius R_0 with a constant vorticity density Ω_0 is used as an initial state of the vortex structure. Figure 1 shows the thus symmetrized initial flow in a model cell. The calculations are performed for the following values of the parameters: $\alpha = \mu_b/\mu = 0$–2, $\beta = \Omega_0 R_0/(2U_0) = 0.2$–$0.5$, $\chi = l/(2R_0) = 2$–6, $\mathrm{M}_0 = U_0/\sqrt{\gamma RT_0} = 0.2$–$0.8$, $\mathrm{Re} = 2U_0R_0\rho_0/\mu = 40$–$100$, and the Prandtl number $\mathrm{Pr} = \mu c_p/\lambda = 0.74$.

2. Governing Equations and Method of the Solution. 2.1. *Initial Boundary-Value Problem.* The structure evolution in the model cell is described by a system of full Navier–Stokes equations for a compressible viscous heat-conducting gas. Calculations make it possible to analyze energy and momentum exchange between the disturbance and the main flow, which occurs both at the loss of stability and in the course of turbulence generation. The reference values chosen for normalization are the initial diameter of the structure $2R_0$, the absolute value of velocity U_0, the density ρ_0, the temperature T_0 on the upper and lower boundaries of the model cell, the time $\tau_0 = 2R_0/U_0$, and the pressure $p_0 = \rho_0 U_0^2$.

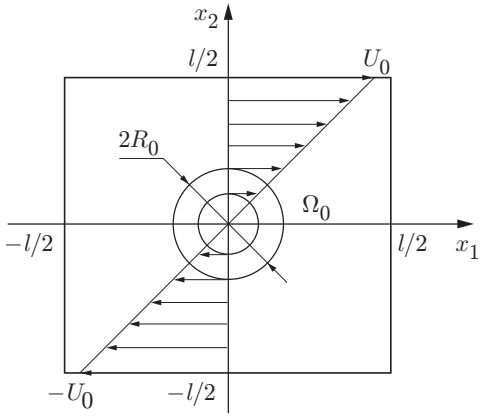

Fig. 1. Flow pattern at the initial time.

In dimensionless variables, the system of equations is written as

$$\frac{\partial \rho}{\partial t} + \frac{\partial \rho u_i}{\partial x_i} = 0,$$

$$\rho\Big(\frac{\partial u_i}{\partial t} + u_j\,\frac{\partial u_i}{\partial x_j}\Big) = -\frac{\partial p}{\partial x_i} + \frac{1}{\mathrm{Re}}\,\frac{\partial^2 u_i}{\partial x_j^2} + \frac{1}{\mathrm{Re}}\Big(\alpha + \frac{1}{3}\Big)\frac{\partial^2 u_j}{\partial x_i\,\partial x_j},$$

$$\rho\Big(\frac{\partial T}{\partial t} + u_i\,\frac{\partial T}{\partial x_i}\Big) = (\gamma-1)\mathrm{M}_0^{\,2}\,\frac{dp}{dt} + \frac{1}{\mathrm{Re\ Pr}}\,\frac{\partial^2 T}{\partial x_i^2} + \frac{(\gamma-1)\mathrm{M}_0^{\,2}}{2\,\mathrm{Re}}\Big(\frac{\partial u_i}{\partial x_j} + \frac{\partial u_j}{\partial x_i}\Big)^2 + (\gamma-1)\Big(\alpha - \frac{2}{3}\Big)\frac{\mathrm{M}_0^{\,2}}{\mathrm{Re}}\Big(\frac{\partial u_i}{\partial x_i}\Big)^2, \tag{7}$$

$$\gamma \mathrm{M}_0^2 p = \rho T, \qquad \frac{d}{dt} = \frac{\partial}{\partial t} + u_i\,\frac{\partial}{\partial x_i}, \qquad i,j = 1,2.$$

On the cell boundaries, the following conditions are satisfied at all times: for $x_1 = \pm\chi/2$ and $x_2 \in [-\chi/2;\chi/2]$,

$$\begin{gathered} u_1(t,\chi/2,x_2) = u_1(t,-\chi/2,x_2), \qquad u_2(t,\chi/2,x_2) = -u_2(t,-\chi/2,x_2), \\ \rho(t,\chi/2,x_2) = \rho(t,-\chi/2,x_2), \qquad p(t,\chi/2,x_2) = p(t,-\chi/2,x_2); \end{gathered} \tag{8}$$

for $x_2 = \pm\chi/2$ and $x_1 \in [-\chi/2;\chi/2]$,

$$\begin{gathered} u_1(t,x_1,\chi/2) = -u_1(t,x_1,-\chi/2), \qquad u_2(t,x_1,\chi/2) = u_2(t,x_1,-\chi/2), \\ \rho(t,x_1,\chi/2) = \rho(t,x_1,-\chi/2), \quad p(t,x_1,\chi/2) = p(t,x_1,-\chi/2). \end{gathered} \tag{9}$$

The carrier flow in the calculation domain is specified as an exact stationary solution of system (7) with boundary values depending on x_1 and x_2 similarly to (8) and (9). In dimensionless variables, the profiles of velocity, temperature, and density are written as

$$U_2(x_2) = \frac{2x_2}{\chi}, \quad T(x_2) = 1 + \frac{(\gamma-1)\mathrm{M}_0^{\,2}\mathrm{Pr}}{2}\Big(1 - \frac{4x_2^2}{\chi^2}\Big), \quad \Theta(x_2) = T^{-1}(x_2). \tag{10}$$

At the same time, as follows from (7) and from the equation of state, the pressure in such a flow is constant over the space: $P = 1/(\gamma \mathrm{M}_0^{\,2})$.

The initial conditions for the velocity field are given in the form

$$\begin{gathered} u_1(0,x_1,x_2) = \begin{cases} 2x_2/\chi + \beta x_2/(2r^2), & r > 1/2, \\ 2x_2/\chi + 2\beta x_2, & r \leqslant 1/2, \end{cases} \\ u_2(0,x_1,x_2) = \begin{cases} -\beta x_1/(2r^2), & r > 1/2, \\ -2\beta x_1, & r \leqslant 1/2, \end{cases} \end{gathered} \tag{11}$$

where $r = \sqrt{x_1^2 + x_2^2}$. The initial distributions of thermodynamic quantities correspond to the conditions of an undisturbed carrier flow (10).

2.2. *Integral Equations of Balance.* In calculating the nonlinear interaction of the disturbance with the main flow, integral equations of balance between bilinear fluctuating characteristics and the kinetic energy of the disturbance are used. To derive these equations within the scope of this model problem, instantaneous values of hydrodynamic quantities are presented as

$$u_i = U_i + u_i', \qquad p = P + p', \qquad \rho = \Theta + \rho'. \tag{12}$$

In (12), a stationary solution U_i, P, and Θ of the system of Navier–Stokes equations (carrier flow) and the imposed disturbance satisfying conditions (8), (9) are singled out. The carrier flow is assumed to be one-dimensional and depend only on the transverse coordinate x_2, i.e., $U_1 = U_1(x_2)$. It is considered that the velocity disturbance in the vicinity of the calculation cell satisfies the conditions

$$\begin{gathered} u_1'(t, x_1, x_2) = u_1'(t, -x_1, x_2), \qquad u_2'(t, x_1, x_2) = -u_2'(t, -x_1, x_2), \\ u_1'(t, x_1, x_2) = -u_1'(t, x_1, -x_2), \qquad u_2'(t, x_1, x_2) = u_2'(t, x_1, -x_2). \end{gathered} \tag{13}$$

By substituting (12) into system (7) and by eliminating terms related to the stationary solution, we obtain the following equations for disturbances with unrestricted amplitudes:

$$\frac{\partial \rho'}{\partial t} + u_i \frac{\partial \rho}{\partial x_i} + \rho \frac{\partial u_i'}{\partial x_i} = 0; \tag{14}$$

$$\rho\Big(\frac{\partial u_i'}{\partial t} + u_j' \frac{\partial u_i'}{\partial x_j} + U_j \frac{\partial u_i'}{\partial x_j} + u_j' \frac{\partial U_i}{\partial x_j}\Big) + \rho' U_j \frac{\partial U_i}{\partial x_j} = -\frac{\partial p'}{\partial x_i} + \frac{1}{\mathrm{Re}} \frac{\partial^2 u_i'}{\partial x_j^2} + \frac{1}{\mathrm{Re}} \Big(\alpha + \frac{1}{3}\Big) \frac{\partial^2 u_j'}{\partial x_i \, \partial x_j}, \quad i, j = 1, 2. \tag{15}$$

By multiplying Eq. (15) by the fluctuating component of velocity u_k' and performing symmetrization over indices, we obtain the equation for bilinear fluctuations

$$\begin{gathered} \frac{\partial}{\partial t} (\rho u_i' u_k') + \frac{\partial}{\partial x_j} (\rho u_j' u_i' u_k') + \frac{\partial}{\partial x_j} (\rho u_i' u_k' U_j) + (\rho u_j' + \rho' U_j)\Big(u_k' \frac{\partial U_i}{\partial x_j} + u_i' \frac{\partial U_k}{\partial x_j}\Big) \\ = -\Big(u_k' \frac{\partial p'}{\partial x_i} + u_i' \frac{\partial p'}{\partial x_k}\Big) + \frac{1}{\mathrm{Re}}\Big(u_k' \frac{\partial^2 u_i'}{\partial x_j^2} + u_i' \frac{\partial^2 u_k'}{\partial x_j^2}\Big) + \frac{1}{\mathrm{Re}}\Big(\alpha + \frac{1}{3}\Big)\Big(u_k' \frac{\partial}{\partial x_i} + u_i' \frac{\partial}{\partial x_k}\Big) \frac{\partial u_j'}{\partial x_j}. \end{gathered} \tag{16}$$

In the left side of Eq. (16), terms in the divergent form are found using the equation of continuity (14). By integrating equation (16) over the calculation domain with allowance for conditions (8), (9), and (13), we obtain the integral equation for bilinear fluctuating characteristics

$$\begin{gathered} \frac{d}{dt} \int\limits_\Omega (\rho u_i' u_k') \, d\Omega = -\int\limits_\Omega \rho u_j' \Big(u_i' \frac{\partial U_k}{\partial x_j} + u_k' \frac{\partial U_i}{\partial x_j}\Big) \, d\Omega + \int\limits_\Omega p' \Big(\frac{\partial u_k'}{\partial x_i} + \frac{\partial u_i'}{\partial x_k}\Big) \, d\Omega \\ - \frac{2}{\mathrm{Re}} \int\limits_\Omega \Big(\frac{\partial u_i'}{\partial x_j} \frac{\partial u_k'}{\partial x_j}\Big) \, d\Omega - \frac{1}{\mathrm{Re}}\Big(\alpha + \frac{1}{3}\Big) \int\limits_\Omega \Big(\frac{\partial u_k'}{\partial x_i} + \frac{\partial u_i'}{\partial x_k}\Big) \frac{\partial u_j'}{\partial x_j} \, d\Omega, \qquad i, j, k = 1, 2. \end{gathered} \tag{17}$$

By convolving Eq. (17) over indices for $i = k$, we obtain an integral equation of balance for the kinetic energy of disturbances

$$\frac{dE}{dt} \equiv \frac{d}{dt} \int\limits_\Omega \frac{\rho u_i'^2}{2} \, d\Omega = J_1 + J_2 - \frac{1}{\mathrm{Re}} (J_3 + \alpha J_4). \tag{18}$$

The term

$$J_1 = -\int\limits_\Omega \rho u_i' u_j' \frac{\partial U_i}{\partial x_j} \, d\Omega$$

describes the energy exchange between the disturbance (structure) and the main flow. The integral

$$J_2 = \int\limits_\Omega p' \frac{\partial u_i'}{\partial x_i} \, d\Omega$$

can be interpreted as the work under fluctuating compression (expansion) of the gas. The integrals

$$J_3 = \int\limits_\Omega \Big[\Big(\frac{\partial u_i'}{\partial x_j}\Big)^2 + \frac{1}{3}\Big(\frac{\partial u_i'}{\partial x_i}\Big)^2\Big]\, d\Omega, \qquad J_4 = \int\limits_\Omega \Big(\frac{\partial u_i'}{\partial x_i}\Big)^2\, d\Omega$$

correspond to dissipation processes.

It must be noted that integrals on the model-cell boundaries, emerging in deriving the integral equations, rigorously vanish for the chosen boundary conditions.

If averaging over the cell area $|\Omega|$

$$\langle G\rangle = \frac{1}{|\Omega|}\int\limits_\Omega G\, d\Omega$$

is introduced, then Eq. (18) can be treated as an equation for averaged characteristics within a constant factor.

In the expressions above, the signs of the integrals J_1 and J_2 are not defined, whereas J_3 and J_4 are nonnegative. It follows from Eq. (18) that the bulk and dynamic viscosities promote disturbance suppression in the case of nonlinear interaction of the structure with the main flow.

It can be noted that Eq. (18), after a certain modification of the main flow profile and boundary conditions, makes it possible to formulate a variational problem for estimating the critical transition Reynolds number $\mathrm{Re}_{\mathrm{cr}}$, which, for $dE/dt = 0$, is calculated as the minimum of the functional

$$\mathrm{Re}_{\mathrm{cr}} = \min\Big[\frac{J_3 + \alpha J_4}{J_1 + J_2}\Big].$$

As follows from (18), for each value of $\mathrm{Re} < \mathrm{Re}_{\mathrm{cr}}$, the dissipative terms J_3 and J_4 prevail, and the derivative $dE/dt < 0$ and all disturbances decay with time. Consequently, the increase in bulk viscosity (or in the parameter α) really shifts the transition to higher values of $\mathrm{Re}_{\mathrm{cr}}$, but a quantitative result can be obtained only by solving the variational problem.

2.3. *Difference Scheme.* In numerical calculations, system (7) is approximated by a weighting finite-difference scheme with splitting in terms of spatial coordinates and physical processes [14]. In the operator form, the scheme is written as

$$(\boldsymbol{x}^{n+1} - \boldsymbol{x}^n)/\tau + L_h[\delta\boldsymbol{x}^{n+1} + (1-\delta)\boldsymbol{x}^n] = \boldsymbol{F}_h^n. \tag{19}$$

Here $\boldsymbol{x}^n = (\rho_{ij}^n, u_{1,ij}^n, u_{2,ij}^n, T_{ij}^n)$ is the grid vector function of the solution in the nth time layer, h is the step of the space grid, τ is the time step, and δ is the weighting parameter. The operator L_h includes symmetric second-order approximations of the first and second spatial derivatives along each spatial coordinate. The operator $\boldsymbol{F}_h^n$ is treated as a vector of right sides and is composed of second-order approximations symmetric about each coordinate of mixed derivatives from equations of momenta and the terms of the dissipative function from the energy equation. On a regular grid with a step h along both coordinates, scheme (19) approximates system (7) with an order $O(\tau + h^2)$ and is absolutely stable for the weighting parameter $\delta > 1/2$ [14].

In the calculation domain, the grid contained $31 \times 31 = 961$ nodes with a step $h = 0.1$. The time step was $\tau = 0.01$. The disturbance evolution was observed until it reached the cell boundary, which required up to 600 time steps.

2.4. *Test Calculations.* The effect of additional disturbance suppression due to bulk viscosity was preliminarily estimated as several percent. Therefore, the calculation errors have to be lower than the third order of smallness. To reach such a result, the difference scheme was always carefully tested. In particular, scheme (19) had to retain a stationary carrier flow (10) in the absence of an imposed disturbance. At the times $(600–800)\tau$, deviations from the stationary profiles of hydrodynamic quantities practically did not exceed the rounding error, remaining at the level $\varepsilon_s = 10^{-6}$.

In addition, in the absence of the carrier flow, the difference problem (19) was solved with the initial-boundary conditions (8), (9), and (11). By virtue of the problem symmetry, the velocity-field divergence is zero. On the assumption of an isochoric process with $\rho = \mathrm{const}$, the continuity equation is satisfied identically. The evolution of the initial disturbance in the form of the Rankine vortex is described by the well-known analytical solution for a viscous incompressible fluid [2]. According to the introduced notation, the expression for the vorticity field has the form

$$\omega(r,\,t)=\frac{\beta\chi\,\mathrm{Re}}{t}\,\exp\Big(-\frac{r^2\,\mathrm{Re}}{4t}\Big)\int\limits_0^{1/2}\exp\Big(-\frac{\xi^2\,\mathrm{Re}}{4t}\Big)\,I_0\Big(\frac{r\,\mathrm{Re}}{2t}\,\xi\Big)\,\xi\,d\xi, \tag{20}$$

where $I_0(\zeta)$ is the zero-order Bessel function of the second kind of the imaginary argument and $r=\sqrt{x_1^2+x_2^2}$ is the distance from the vortex center to an arbitrary point of the calculation cell.

In the numerical solution, the grid vorticity function is calculated on the basis on the symmetrical finite-difference approximation

$$\omega_{ij}^n=\frac{\chi}{2}\Big(\frac{u_{1,\,i,j-1}^n-u_{1,\,i,j+1}^n}{2h}-\frac{u_{2,\,i-1,j}^n-u_{2,\,i+1,j}^n}{2h}\Big). \tag{21}$$

In the range of examined parameters used, the maximum difference between the calculated values (21) and the analytical solution (20) in all grid nodes did not exceed the value $\varepsilon_d=5\cdot10^{-3}$ in the time interval up to 600τ.

For testing the scheme accuracy for $\rho\neq\mathrm{const}$, the coincidence between the time evolution of vorticity at the center of the Rankine vortex in compressible and incompressible viscous fluids was used. The respective analytical solution for the vorticity is given by the formula [2]

$$\omega(0,t)=2\beta\chi(1-\exp\left(-\,\mathrm{Re}\,/(16t)\right)).$$

As the calculation shows, in this case, the maximum difference of the numerical solution at the center of the model cell from this analytical expression does not exceed the value $\varepsilon_d=5\cdot10^{-3}$ in the time interval of up to 600τ either.

The test results confirm that the numerical model developed ensures sufficient accuracy of the problem solution.

3. Calculation Results and Their Discussion. The energy exchange between the carrier flow and disturbances of various space and time scales is one of the basic processes both in the laminar–turbulent transition and in developed turbulence. To estimate the influence of bulk viscosity on fluctuating characteristics of the model flow, we investigated the time evolution of absolute values of the Reynolds stresses

$$\sigma_{12}(t)=\int\limits_{-\chi/2}^{\chi/2}\int\limits_{-\chi/2}^{\chi/2}|\rho u_1'u_2'|\,dx_1\,dx_2 \tag{22}$$

and the kinetic energy of disturbances

$$E(t)=\frac{1}{2}\int\limits_{-\chi/2}^{\chi/2}\int\limits_{-\chi/2}^{\chi/2}\rho(u_1'^2+u_2'^2)\,dx_1\,dx_2. \tag{23}$$

The integrands in (22) and (23) were calculated from instantaneous flow characteristics obtained from the numerical solution of system (7) using the difference scheme (19). The integrals were calculated by the rectangle formula on a regular grid with a step $h=0.1$.

An example of calculating the dependences $E(t)$ for $\alpha=0$–2 is shown in Fig. 2a. The dependences $\sigma_{12}(t)$ have a similar character. Figure 2b shows the curves $\sigma_{12}(\alpha)$ at various times θ. On averaging over the same time intervals in the form,

$$\langle F(\alpha)\rangle=\theta^{-1}\int\limits_0^{\theta}F(t,\alpha)\,dt$$

the dependences $\langle E(\alpha)\rangle$ and $\langle\sigma_{12}(\alpha)\rangle$ become less steep than those in Fig. 2b, although retaining their character. The order of magnitude of the time interval up to $\theta=5$ corresponds to the average lifetime of a large structure. At this moment, in the calculations, the disturbance level on the boundary reached the value of the numerical calculation error, after which the computation was stopped.

As follows from the presented plots, as the coefficient of bulk viscosity grows, the kinetic energy of disturbances and the Reynolds stresses decay more intensively. The maximum stratification of the curves $E(t)$ and the most drastic change in $\sigma_{12}(\alpha)$ are observed at $\theta=4$–5. In order to estimate the effect of bulk viscosity on the average fluctuating characteristics, the relative changes

$$\Delta_F=|\langle F(\alpha)\rangle-\langle F(0)\rangle|/\langle F(0)\rangle \tag{24}$$

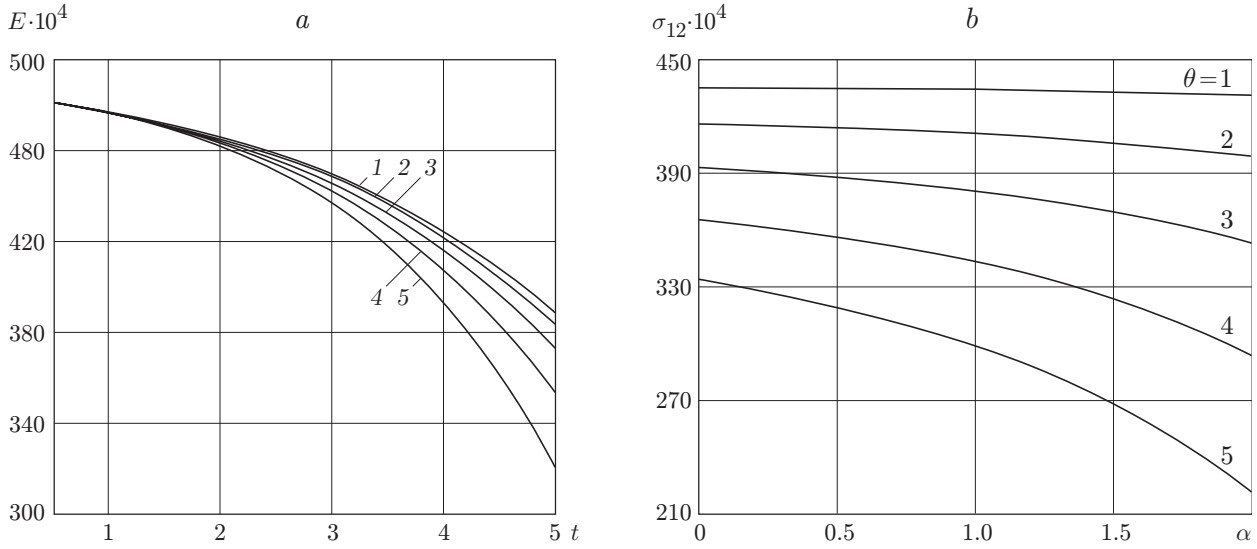

Fig. 2. Effect of bulk viscosity disturbance evolution (Re = 100, Pr = 0.74, $M_0 = 0.5$, $\beta = 0.2$, $\chi = 3$, and $\gamma = 1.4$): (a) kinetic energy versus time for $\alpha = 0$ (1), 0.5 (2), 1 (3), 1.5 (4), and 2 (5); (b) absolute values of the Reynolds stresses σ_{12} versus the parameter α (or μ_b) at different times θ.

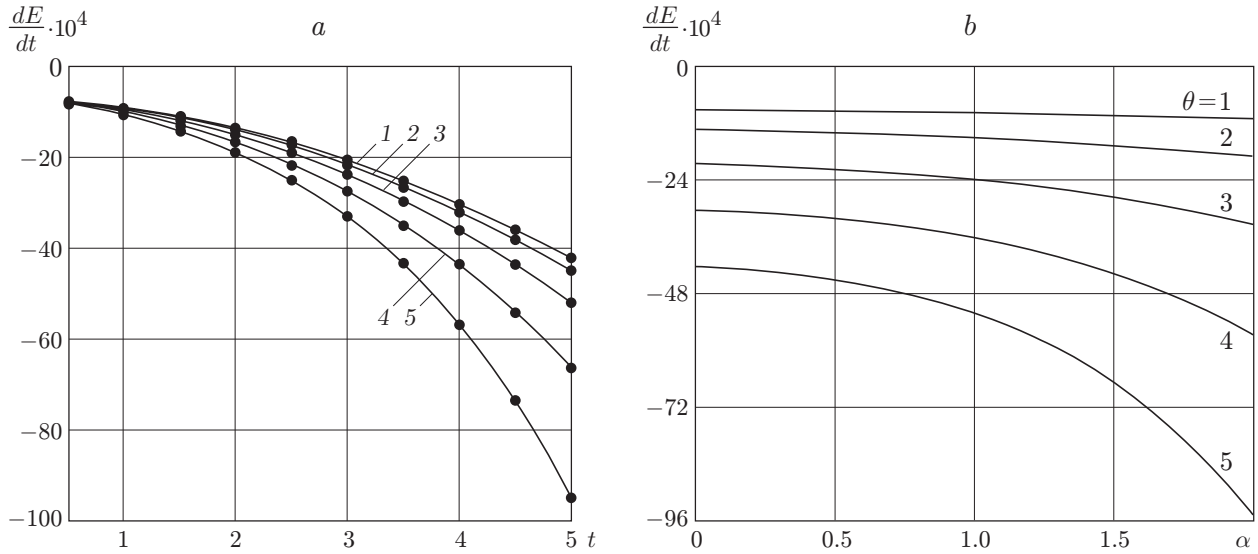

Fig. 3. Generation of kinetic energy of disturbances: (a) versus time [the curves are constructed on the basis of the calculation results of Eq. (18); the points refer to the calculation results of Eqs. (23) and (25)]; (b) versus bulk viscosity at different times θ (the regime parameters and notation employed are the same as in Fig. 2.)

for the time interval $0 \leqslant \theta \leqslant 5$ were calculated. For the calculation conditions corresponding to Fig. 2, both for the kinetic energy $\langle E(\alpha)\rangle$ and for the absolute value of the Reynolds stresses $\langle\sigma_{12}(\alpha)\rangle$, the characteristic Δ_F changes in the range from 0.012 to 0.096 for $\alpha = 0.5$–2.0. As the Mach number increases, the both limits proportionately grow, and the upper limit reaches the value $\Delta_F \simeq 0.2$ for $M_0 = 2$. However, for this value of M_0, the above-chosen parametrization of the model flow, and the model of bulk viscosity itself, can prove useless.

In the mixing layer, the contribution of organized vortices to the total Reynolds stresses and kinetic energy of fluctuations is known to be approximately 40% [12]. It is obvious, at the same time, that molecular dissipation suppresses small-scale disturbances much more intensively than large-scale disturbances considered here. Proceeding from this fact, the calculated changes in the value of Δ_F ($\Delta_F \leqslant 0.1$) may be extended to the entire spectrum of disturbances.

On the basis of the discrete approximation of Eq. (18), the time evolution of the kinetic energy $dE(t)/dt$ is calculated. The respective plots are shown in Fig. 3. In order to test the calculation accuracy, the finite-difference approximation

$$\frac{dE}{dt} \simeq \frac{E(t+\tau) - E(t-\tau)}{2\tau} \tag{25}$$

is calculated parallel to the calculations by Eq. (18). Scattering of the data obtained by two methods does not exceed 1%. It is obvious that, with increasing parameter α, the absolute value of the kinetic energy dissipation rate increases. The dissipation rate also grows with time. The time-averaged dependences $\langle dE/dt \rangle$ (Fig. 3a) have lower gradients than the curves in Fig. 3b; at the same time, the character of the dependences remains unchanged. As the Mach number grows, the influence of bulk viscosity on the dissipation rate becomes stronger. We can state that the relative increments for the averaged values of $\langle dE/dt \rangle$ calculated from relation (18) are within the same limits as for the kinetic energy of disturbances.

An analysis of the calculation results shows that generation of kinetic energy of fluctuations in this model problem is always negative. The absence of a mechanism for positive generation of disturbance energy, for instance, such as expansion of quasi-streamwise vortices connecting large structures in the mixing layer [12], is a drawback of a simplified two-dimensional model preventing its application to immediate estimation of the effect of bulk viscosity μ_b on the critical transition Reynolds number.

Conclusions. On the basis of a simple model, the influence of bulk viscosity on the nonlinear interaction of a finite-amplitude vortex disturbance with a carrier shear flow is studied. The range of parameters of the model flow corresponds to the real values for molecular gases. Numerical modeling results seem to evidence a stabilizing effect of bulk viscosity on the dynamics of disturbances. It is shown that, in a weakly compressible flow with $\mathrm{M}_0 < 1$, as bulk viscosity increases in the range $0 \leqslant \mu_b \leqslant 2\mu$, the relative decrease in the absolute value of the Reynolds stresses and kinetic energy of disturbances increase and approach 10% for $\mu_b = 2\mu$. The results obtained are not final and require further investigation based on improved and more perfect models. It should be noted, at the same time, that such a suppression of fluctuating intensity can be achieved by means of well-known mechanical methods for drag reduction, for instance, by ribleting surfaces in the flow [5]. Therefore, the results point to a hypothetical possibility of drag control in compressible flows by regulating bulk viscosity of the gas. In particular, it can be done via laser pumping of vibrational levels of gas molecules.

This work was partly supported by the Russian Foundation for Fundamental Research (Grant No. 01-01-00827).

REFERENCES

1. M. A. Leontovich, "Notes on the theory of sound absorption in gases," *Zh. Éksp. Teor. Fiz.*, **6**, No. 6, 561–576 (1936).
2. N. E. Kochin, I. A. Kibel, and N. V. Rose, *Theoretical Hydromechanics* [in Russian], Part 2, Fizmatgiz, Moscow (1963).
3. L. M. Mack, "Boundary layer stability theory," Pasadena, California (1969). (Rev. A, Jet Propulsion Lab., Doc. No. 900-277.)
4. A. Nerushev and S. Novopashin, "Rotational relaxation and transition to turbulence," *Phys. Lett.*, **A232**, 243–245 (1977).
5. A. M. Savill, "Drag reduction by passive devices — a review of some recent developments," in: A. Gyr (ed.), *Structure of Turbulence and Drag Reduction*, Springer Verlag, Berlin etc. (1990), pp. 429–465.
6. F. B. Bertolotti, "The influence of rotational and vibrational energy relaxation on boundary-layer stability," *J. Fluid Mech.*, **372**, 93–118 (1998).
7. S. A. Gaponov and A. A. Maslov, *Development of Disturbances in Compressible Flows* [in Russian], Nauka, Novosibirsk (1980).
8. Yu. N. Grigor'ev and I. V. Ershov, "On rotational relaxation effect on laminar-turbulent transition," in: *Proc. of the Commemorative Conference Devoted to the* 40*th Anniversary of the Institute of Mechanics at the Moscow University* (Moscow, November 22–26, 1999), Izd. Mosk. Univ., Moscow (1999), pp. 65–66.
9. I. S. Grigor'ev and Ye. Z. Meilikhov (eds.), *Physical Quantities: Handbook* [in Russian], Énergoatomizdat, Moscow (1991).

10. V. M. Zhdanov and M. Ya. Alievskii, *Transport and Relaxation Processes in Molecular Gases* [in Russian], Nauka, Moscow (1989).
11. C. A. Brau and R. H. Johnkman, "Classical theory of rotational relaxation in diatomic gases," *Phys. Fluids*, **52**, 477–484 (1970).
12. F. K. Browand and Chih Ming Ho, "The mixing layer: An example of quasi two-dimensional turbulence," *J. Mechanique Teor. Appl.*, Spec. nr., 99–120 (1983).
13. G. N. Abramovich, T. A. Girshovich, S. Yu. Krasheninnikov, et al., *Theory of Turbulent Jets* [in Russian], Nauka, Moscow (1984).
14. V. M. Kovenya and N. N. Yanenko, *Splitting Method in Problems of Gas Dynamics* [in Russian], Nauka, Novosibirsk (1981).